

IMPROVED METHOD TO DETERMINE THE HARDNESS AND ELASTIC MODULI USING NANO-INDENTATION

Nurot Panich*, Sun Yong
School of Materials Engineering,
Nanyang Technological University, Republic of Singapore, 639798

ABSTRACT

It is well known that hardness and elastic moduli can be determined by indenting the specimen to various depths. This paper shows the application of three approximation approaches for this purpose: the ideal method, Sun's method, and modified Oliver & Pharr's method. A comparison of the results for silicon (100) and high speed steel (HSS) specimens in terms of hardness and elastic moduli has been made. In general, the results obtained from the Sun's method are more stable and reliable than the other methods.

KEYWORDS: Nanoindentation, load-displacement curve, hardness

1. INTRODUCTION

Recently, many efforts have been made in developing nanoindentation equipment and nanoindentation techniques for probing the mechanical properties of materials and thin film on the sub-micron and nano-scale [1-4]. The most extensively used method to determine the elastic moduli and hardness by nanoindentation was proposed by Oliver and Pharr [5], in which the slope of the unloading curve which is usually nonlinear was used to calculate the elastic moduli and to provide a physically justifiable procedure for determining the depth which should be used in conjunction with the indenter shape function to establish the contact area at peak load.

2. THEORY OF NANOINDENTATION

Nanoindentation test involves indenting a specimen by a very small load using a high precision instrument, which records the load and displacement continuously. The mechanical properties of thin films coatings and substrates can be derived from the measure load-displacement loading/unloading curve through appropriate data analysis. These tests are based on new technologies that allow precise measurement and control of the indenting forces and precise measurement of the indentation depths [6].

In nanoindentation, a prescribed load is applied to a pyramidal or spherical indenter or other shapes in contact with the specimen surface. As load is applied to the indenter, the depth of penetration into the specimen is measured. A nanoindentation test instrument provides experimental results in the form of a load-displacement curve for the loading and the unloading parts of the indentation process as shown in Figure 1. An analysis of the unloading data provides a value for the depth of the circle of contact at full load. The area of contact at full load is determined from the known angle or radius of the indenter. The hardness is derived by dividing the load by the area of contact. The slope of the unloading curve provides a measure of elastic moduli [7]. To make accurate measurements by indentation experiments, the contact areas of the indentations must be precisely known.

* Corresponding author. Fax: (65) 6790-9081; Email: panich@pmail.ntu.edu.sg

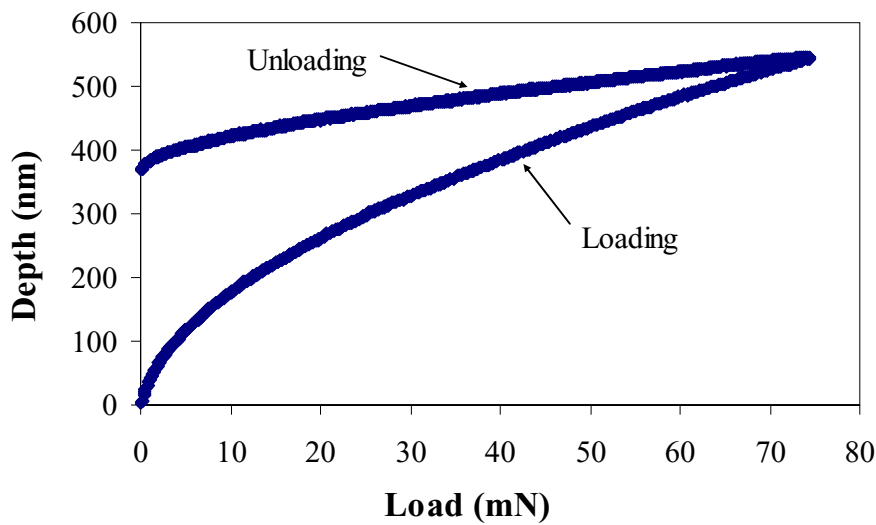


Figure 1 Nanoindentation load–displacement curve for high speed steel obtained with a Berkovich indenter during loading and unloading

The most popular calibration technique is that of Oliver and Pharr [5] which is based on the elastic solution of Sneddon [8] for indentation by an axisymmetric body. Sneddon derived general relationships between load and displacement for many simple punch geometries, written as;

$$P = Kh_c^m \tag{1}$$

where P is the indentation load, h_c is the measured depth, and K and m are constants. Values of the exponent m for some common punch geometries are $m = 1$ for flat cylinders, $m = 2$ for cones, $m = 1.5$ for spheres and $m = 1.5$ for paraboloids. The proportional constant K is determined by materials properties and indenter geometry. Sun, Bell and Smith [unpublished] and Hainsworth [9] have shown that, for the specified perfectly sharp indenter, K is mainly determined by Young’s moduli and the hardness of the indenting material. So far, experiments have shown that indentation loading curves obtained with Berkovich indenters ($m = 2$) are usually well-described by equation (1).

Because the displacements during unloading are elastic, the relationship between the unloading curve and the elastic moduli of the material being tested can be described by elastic contact theory. Pharr *et al.* [10] have shown that the compliance of the contact between any axisymmetric indenter and an elastically isotropic half-space is given by

$$\frac{1}{S} = C_s = \frac{dh}{dP} = \frac{\sqrt{\pi}}{2} \cdot \frac{1}{\sqrt{A}} \cdot \frac{1}{E_r} \tag{2}$$

$$\frac{1}{E_r} = \frac{(1 - \nu_s^2)}{E_s} + \frac{(1 - \nu_i^2)}{E_i} \tag{3}$$

where S is the experimentally measured stiffness of unloading data, A is the projected area of the contact, C_s is the specimen’s compliance and P is the load on the indenter. E_r is the

reduced moduli owing to the effects of elastic deformation of indenter (non-rigidity) and is the combined Moduli of the indenter and the specimen. E_s , ν_s , E_i and ν_i are the elastic moduli and Poisson's ratio of the specimen and indenter, respectively (here taken to be 1,141 GPa and 0.07 for diamond). Equation (2) has its origins in elastic contact theory and many investigators accept that it can be applied to any indenter that can be described as a body of revolution of a smooth function. In the usual way we define the hardness of the material, H , to be the mean pressure exerted by the indenter at maximum load,

$$H = \frac{P_{\max}}{A} \tag{4}$$

where P_{\max} is the maximum load applied during the indentation and A is the projected area of contact between the indenter and the specimen. The measurements of indentation moduli and hardness depend on knowing the contact area of the indentations. For an ideally sharp Berkovich indenter the cross-sectional area in terms of contact depth is expressed as follows:

$$A(h_c) = 24.5h_c^2 \tag{5}$$

However, in reality all indenters have a certain degree of roundness and imperfection, as shown in Figure 2. The area function of the actual indenter tip must therefore be calibrated experimentally.

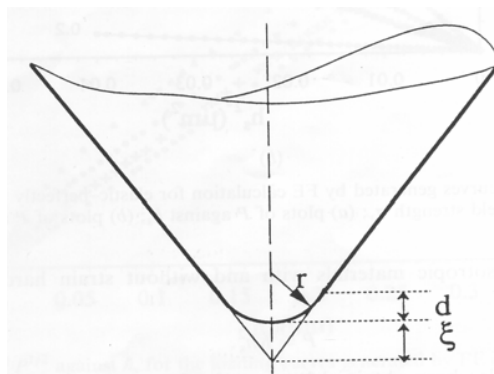


Figure 2 Schematic diagram showing the geometry of a round tip indenter

From Figure 2, the correction depth, ξ , is the difference in depth between the ideally sharp tip and the round tip of radius r .

Oliver & Pharr [5] proposed a method to calibrate the load frame compliance and area function by using unloading curves to derive the overall compliance of the specimen and the load frame for each depth. This was based on the assumption that Young's moduli for the sample does not vary with depth, and iteration technique was then used to derive the C_f value for the load frame. The method followed by modeling the load frame and the specimen as two springs in series, in which case

$$C = C_s + C_f \tag{6}$$

where C is the total measured compliance and C_s is the compliance of the specimen. Since the specimen compliance during elastic contact is given by the inverse of the contact stiffness, S , Eqs. (2) and (6) combine to yield

$$C = \frac{\sqrt{\pi}}{2E_r} \cdot \frac{1}{\sqrt{A}} + C_f \tag{7}$$

It is thus seen that if the moduli is constant, a plot of C vs. $A^{-1/2}$ is linear for a given material, and the intercept of the plot is a direct measure of the load frame compliance. Furthermore, the best values of C_f are obtained when the first term on the right-hand side of Eq. (7) is small, i.e., for large indentations.

For the area function of the indenter tip, the method is based on the assumption that the elastic is dependent on indentation depth and specific values for the moduli are not assumed. To find the area function the method took advantage of the fact that relatively large indentations can be made in aluminum because of its low hardness. Furthermore, for the largest indentations the area function for the ideal Berkovich geometry can be used to provide a first estimate of contact area. Initial estimates of C_f and E_r were thus obtained by plotting C vs. $A^{-1/2}$ for the two largest indentations in aluminum. Using these values, contact areas were computed for all indentation sizes by rewriting Eq. (7) as

$$A = \frac{\pi}{4} \cdot \frac{1}{E_r^2} \cdot \frac{1}{(C - C_f)^2} \tag{8}$$

from which an initial guess at the area function was made by fitting the A vs. h_c data to the relationship

$$A(h_c) = 24.5h_c^2 + C_1h_c^1 + C_2h_c^{1/2} + C_3h_c^{1/4} + \dots + C_8h_c^{1/28} \tag{9}$$

where C_1 through C_8 are constants. The lead term describes a perfect Berkovich indenter; the others describe deviations from the Berkovich geometry due to blunting at the tip. On the other hand, this technique is time consuming and involves a series of indentation experiments from small depths to large depths.

Recently, Sun *et al.* [11] propose a technique for accurate and quick determination of the indenter tip radius and load frame compliance by accounting the correction depth ξ . Analyses of the obtained loading curves showed that the load frame compliance of the nanoindentation instrument can be determined from the single loading curve. In an actual indentation experiment, the obtained raw load-depth data during the loading stage can be described by the second-order polynomial dependence of depth on the square root of load, from which the C_f is determined. For a round tip indenter, it is obvious that Eq. (1) no longer holds true. However, as proposed by Cheng and Cheng [12], if the correction depth ξ is taken into account, then Eq. (1) can also be used to describe approximately the loading curve of a round tip indenter indenting an elastic-perfectly plastic material for depths greater than d , the depth at which the sphere of the tip touches the cone, that is for $h_c > d$;

$$P = K(h_c + \xi)^2 \tag{10}$$

then,

$$P^{1/2} = K^{1/2} \cdot h_c + K^{1/2} \cdot \xi. \tag{11}$$

At any time during loading, the total measured displacement (h) is expressed as the sum of the contact depth or the specimen displacement (h_c) and the displacement of the surface at the perimeter of the contact or the load frame displacement (h_s). It then follows;

$$h = h_c + h_s = h_c + PC_f \quad (12)$$

where C_f is the load frame compliance and P is the load on the indenter. In real indentation experiments, the total depth from Eq. (8) is measured by the instrument. Hence, combining Eqs. (11) and (12) leads to (for $h > d$)

$$h = C_f \cdot P + K^{-1/2} \cdot P^{1/2} - \xi \quad (13)$$

Clearly, a plot of the measured total depth h against the square root of the indentation load $P^{1/2}$ results in a second-order polynomial dependence of h on $P^{1/2}$. From the curve of h against $P^{1/2}$ for silicon, obviously, the intercept of the plot is a direct measure of C_f and the last term of polynomial equation is ξ . The area of indenter tip shows in equation (14) by accounting the correction depth ξ (Fig.2) in the ideal method.

$$A = 24.5(h_c + \xi)^2 \quad (14)$$

Another approach for indenter tip area function calibration, which ξ employed by the commercial instrument: NanoTest™ [13], is the modified O&P method which user uses the two first term of the O&P area function, i.e.

$$A = ah_c + bh_c^2 \quad (15)$$

where a and b are constants, which are determined experimentally by following the O&P procedure outlined previously.

3. EXPERIMENT

Silicon (100) and high speed steel (HSS) were chosen as testing samples in this study. In order to eliminate the surface roughness problem, the specimen's surface needs to be prepared. In addition to high speed steel case, it was ground by standard metallurgical silicon-carbide waterproof papers (grid size 180, 320, 800 and 1,000) and polished. The HSS surface was ultrasonically cleaned with acetone at 20 °C for 5 minutes as well.

Silicon and high speed steel were indented by diamond Berkovich indenter in sub-micron or nano-scales. The experiment was performed using the NanoTest™ [12] (Micro Materials Ltd., Wrexham, United Kingdom) at the Surface Engineering Laboratory, School of Materials Engineering, Nanyang Technological University. The NanoTest device measures the movement of a calibrated diamond indenter penetrating into a specimen surface at a controlled loading rate. This device uses a pendulum pivoted on bearings which are essentially frictionless. The indenter used in this work is a Berkovich diamond, a three-sided pyramid, which is widely used for nanoindentation work because it can be machined down very accurately to a very sharp tip with a curvature radius of one half of a nanometer. The NanoTest device is capable of resolutions of the order of 0.1 μ N and 0.1 nm for the load and displacement respectively, depending on the load and displacement ranges used. For the purpose of statistics and reliability, it is recommended to use ten loading/unloading curves in each experiment. The experiment then involved indenting the specimen to ten different peak depths, from 100 to 1,000 nm, and recording the load-displacement data during the loading and unloading stages. Five indents were made at each peak depth to obtain average results. This involved a total of 50 indentation experiments for each specimen.

4. RESULTS AND DISCUSSION

For the silicon specimen, ten peak loads were investigated starting at 2.92 mN and successively increasing the load at 10.76, 18.32, 30.08, 44.78, 61.76, 81.76, 104.14, 127.99, 154.44 mN. The loading/unloading rate was also raised at a value of 1 mN/s for the 2.92 mN indentations as shown in the loading/unloading curves in Figure 3.

For high speed steel, ten peak loads were investigated starting at 3.71 mN and successively increasing the load at 11.14, 21.49, 38.02, 56.10, 74.18, 95.69, 123.02, 150.22, 184.81 mN. The loading and unloading rate was also raised at a value of 1 mN/s for the 3.71 mN indentations as shown in the loading/unloading curves in Figure 4.

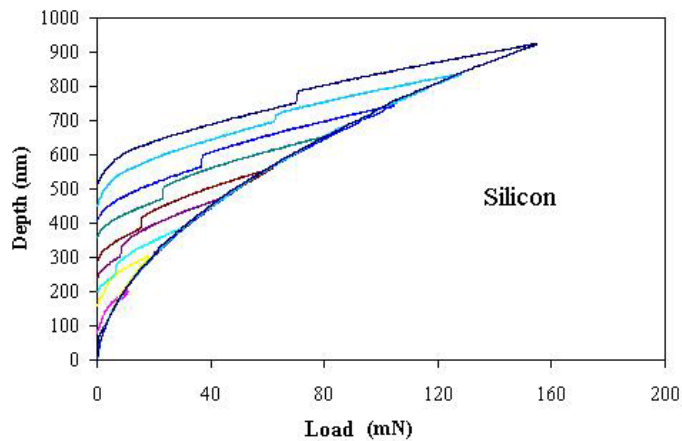


Figure 3 The loading/unloading curves showing ten peak loads of silicon

The hardness and the moduli elastic value of silicon and high speed steel were derived from the indentation unloading curves, using all three methods mentioned above. The contact depth was determined by the O&P procedure, i.e. for fitting the initial part (30% for silicon and 70 % for high speed steel) of the unloading data using the power law function then deriving the tangent of the curve at maximum load.

Figures 5 and 6 show the values of the hardness and reduced moduli of silicon, whilst Figure 7 and Figure 8 show the value of the hardness and reduced moduli of high speed steel, as derived from Sun's method, the modified O&P method and the ideal method.

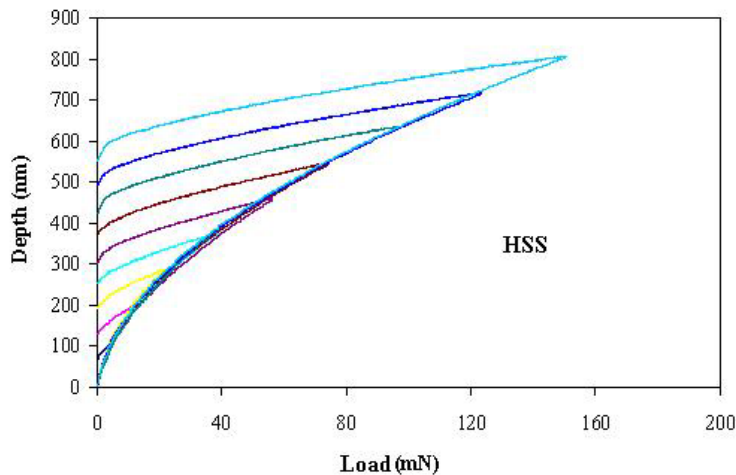


Figure 4 The loading/unloading curves showing ten peak loads of high speed steel

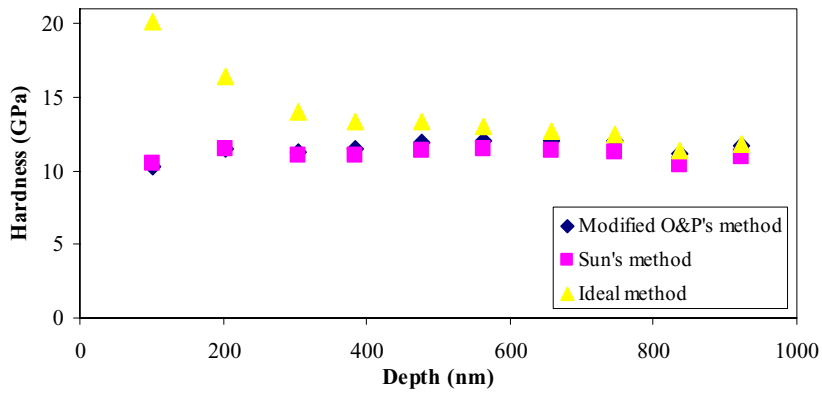


Figure 5 Comparison of the values of the hardness of silicon derived by Sun's method, the modified O&P method and the ideal method

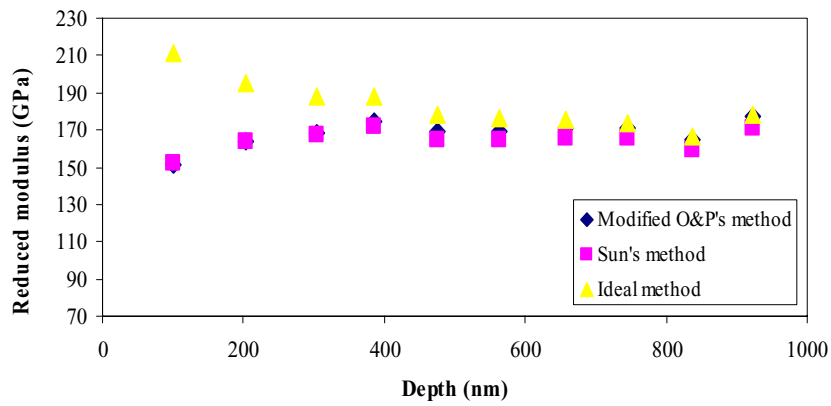


Figure 6 Comparison of the values of the reduced moduli of silicon derived by Sun's method, the modified O&P method and the ideal method

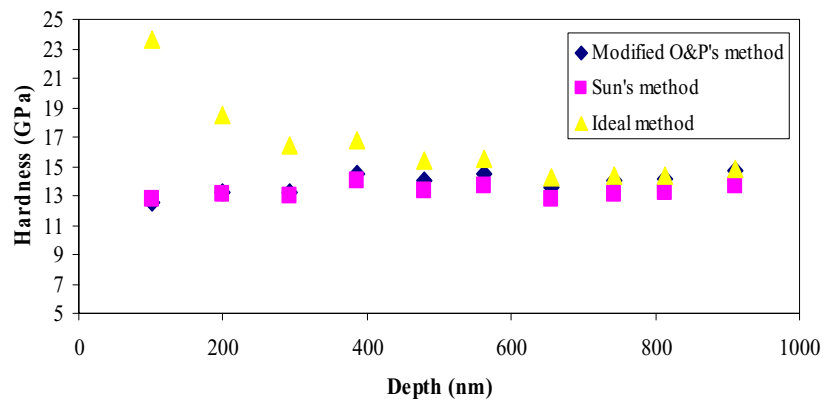


Figure 7 Comparison of the values of the hardness of high speed steel derived by Sun's method, the modified O&P method and the ideal method

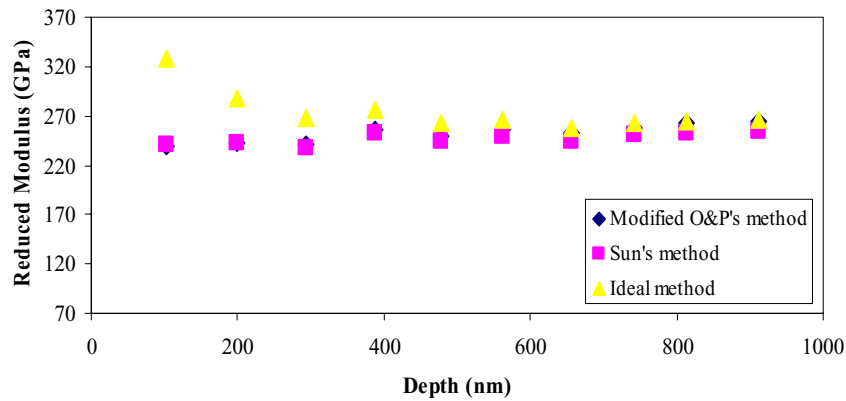


Figure 8 Comparison of the values of the reduced moduli of high sped steel derived by Sun's method, the modified O&P method and the ideal method

Obviously, the values of H and E_r shown in Figures 5-8 show that the Sun's method are more stable than the Ideal method and the modified Oliver and Pharr's method. The values of H and E_r reported in Figures 5-8 significantly drop at low loads. This behavior is normal owing to the fact that the area function obtained by fitting is incorrect at low loads because of the preponderant weight of the measurements done for $P > 20$ mN, as shown in Figure 9. Figure 9 demonstrates the reduced moduli versus the maximum load of silicon and HSS extracted by experiment.

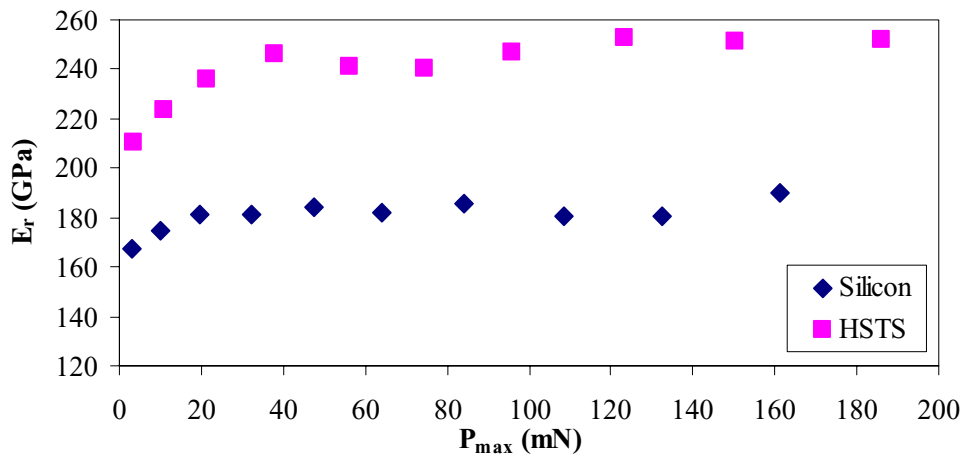


Figure 9 The reduced moduli versus the maximum load of silicon and HSS extracted by experiment

To evaluate the predictive capabilities of the hardness and reduced moduli determination, hardness and reduced moduli obtained by averaging the experimental results of five experiments were compared with commonly accepted values from the literature in Table 1.

Table 1 Comparison of measured hardness and reduced moduli with accepted values in the literature

Material	Method	Experimental		Literature		Poisson's ratio	References
		E (GPa)	H (GPa)	E (GPa)	H (GPa)		
Silicon (100)	Modified O&P's method	154.9	11.5	130 *	11.5 **	0.28	* [14] ** [15]
	Sun's method	151.8	11.1				
	Ideal method	168.7	13.8				
HSS	Modified O&P's method	218.4	13.8	210	67-69 (HRC)	0.30	[16]
	Sun's method	213.9	13.3				
	Ideal method	236.64	16.4				

The table shows that for silicon, the hardness calculated from the experiments are all within 3.5 % of the literature values except the hardness computed from the ideal method which has 20 % error from the literature value. From Table 1, a good agreement between the experiment and the literature hardness indicates that Sun's method and the modified O&P's method work well and reliable. However, the measured reduced moduli is higher than the literature about 16 % for both of Sun's method and the modified O&P's method and about 29 % for the ideal method. This is owing to the high anisotropy of silicon.

For high speed steel, the reduced moduli computed from the experiments are all within 1.8 % error for Sun's method, 3.8 % for the modified O&P's method and 12.6 % for the ideal method of the literature values. From the table, a good agreement between the experiment and the literature hardness then indicates that the Sun's method and the modified O&P's method also work well and may be use to measure the intrinsic mechanical properties of this bulk material. On the other hand, the hardness in the table between the experiment and the literature cannot be compared due to the different references. In this work, all harness values were measured in GPa (10^9), but in the literature used in HRC unit. Nevertheless, a reliable value of the hardness of HSS should be measured from the experiment. In addition, from Table 1, Sun's method and the modified O&P's method show that the hardness of HSS should be 13.3 GPa and 13.8 GPa, respectively.

5. CONCLUSION

Methods to obtain the hardness and reduced moduli from three approaches are presented. Based on the experimental data and results obtained by calculation using, it can be seen that values derived from Sun's method are more stable than the Ideal method and the modified Oliver and Pharr's method. The results of the area function and load frame compliance are crucial to determine the real value of contact area in elastic-plastic region. Thus this novel method (Sun's method) has the potential to determine the precise values of two important mechanical properties.

REFERENCES

- [1] Oliver, W.C., Hutchings, R. and Pathica, J.B. **1986** ASTM STP 889. In: Blau P.J. and Lawn, B.R., Ed. *American Society of Testing and Materials*. Philadelphia, PA, pp. 90-108.
- [2] Doerner, M.F. and Nix, W.D. **1986** A Method for Interpreting the Data from Depth-sensing Indentation Instruments. *Journal of Materials Research*, 1, 601-616.

- [3] Joslin, D.L. and Oliver, W.C. **1990** A New Method for Analyzing Data From Continuous Depth-sensing Microindentation Tests. *Journal of Materials Research*, 5, 123-126.
- [4] Woigard, J. and Dargenton, J-C. **1997** An Alternative Method for Penetration Depth Determination in Nanoindentation Measurements. *Journal of Materials Research*, 12, 2455-2458.
- [5] Oliver, W.C. and Pharr, G.M. **1992** An Improved Technique for Determining Hardness and Elastic Moduli using Load and Displacement Sensing Indentation Experiments. *Journal of Materials Research*, 7, 1564-1583.
- [6] Bell, T.J., Bendeli, A., Field, J.S., Swain, M.V. and Thwaite E.G. **1992** The Determination of Surface Plastic and Elastic Properties by Ultra-Micro Indentation. *Metrologia*, 28, 463-469.
- [7] Fischer-Cripps, A.C. **2000** UMIS II Brochure, CSIRO Telecommunications and Industrial Physics.
- [8] Sneddon, I.N. **1965** The Relation Between Load and Penetration in the Axisymmetric Boussinesq Problem for a Punch of Arbitrary Profile. *International Journal of Engineering Science*, 3, 47.
- [9] Hainsworth, S.V., Chandler, H.W. and Page, T.F. **1996** Analysis of Nanoindentation Load-displacement Loading Curves. *Journal of Materials Research*, 11, 1987-1995.
- [10] Pharr, G.M., Oliver, W.C. and Brotzen, F.R. **1992** On the Generality of the Relationship Between Contact Stiffness, Contact Area, and Elastic Moduli During Indentation. *Journal of Materials Research*, 7, 613-617.
- [11] Sun, Y., Zheng, S., Bell T. and Smith, J. **1999** Indenter Tip Radius and Load Frame Compliance Calibration using Nanoindentation Load Curves. *Philosophica Magazine Letter*, 79, 649-658.
- [12] Cheng, Y.T. and Cheng, C.M. **1998** Further Analysis of Indentation Loading Curves: Effects of Tip Rounding on Mechanical Property Measurements. *Philosophical Magazine Letter*, 77, 39.
- [13] Nano Test-500, Micro Materials Ltd., Wrexham, United Kingdom.
- [14] Peterson. **1982** Silicon as a Mechanical Material. *Proc.IEEE* Vol.7 No.5, pp. 420-475.
- [15] Pharr, G.M. **1998** Measurement of Mechanical Properties by Ultra-low Load Indentation. *Materials Science & Engineering A*, 253, 151-159.
- [16] Ketin, M., Fonderies, S.D. and Marichal K.J. 372 B-4000 Liège (Sclessin), Belgium.